Inorg. Chem. **2007**, *46*, 9873–9883

$[1\text{-}H_2N\text{–}CB_{11}F_{11}]^-$ – Synthesis and Reactions of a Functionalized Fluorinated Carbadodecaborate Anion

Maik Finze,*,† Guido J. Reiss,† and Manfred Zähres‡

Contribution from the Institut für Anorganische Chemie und Strukturchemie II, Heinrich-Heine-Universität Düsseldorf, Universitätsstrasse 1, 40225 Düsseldorf, Germany and the Institut für Physikalische Chemie, Universität Duisburg-Essen, Universitätsstrasse 5, 45141 Essen

Received July 13, 2007

In anhydrous hydrogen fluoride, $K[1\text{-}H_2N\text{–}CB_{11}H_{11}]$ is fluorinated with elemental fluorine to produce $K[1\text{-}H_2N\text{–}CB_{11}F_{11}]$. Under strong alkaline conditions, two fluorine atoms of the $[1\text{-}H_2N\text{–}CB_{11}F_{11}]^-$ anion are regioselectively exchanged, yielding the $[1\text{-}H_2N\text{-}4,6\text{-}(HO)_2\text{–}CB_{11}F_9]^-$ anion via $[1\text{-}H_2N\text{-}6\text{-}HO\text{–}CB_{11}F_{10}]^-$ as an intermediate. Both hydroxycarborate anions were isolated as $[Ph_4P]^+$ salts. All of the species were characterized by IR, Raman, and multi-NMR spectroscopy, thermal analysis (DSC) as well as by mass spectrometry (MALDI). The assignment of the NMR signals was supported by DFT calculations. Solid-state structures of $K[1\text{-}H_2N\text{–}CB_{11}F_{11}]$, $[BzPh_3P][1\text{-}H_2N\text{–}CB_{11}F_{11}]$, $[Ph_4P][1\text{-}H_2N\text{-}4,6\text{-}(HO)_2\text{–}CB_{11}F_9]$, $[Ph_4P][1\text{-}H_2N\text{-}6\text{-}HO\text{–}CB_{11}F_{10}]$, and $[BzPh_3P][1\text{-}H_2N\text{–}CB_{11}H_{11}]$ were determined by single-crystal X-ray diffraction.

Introduction

Highly fluorinated *closo*-carborate anions, $[1\text{-}R\text{-}CB_{11}F_{11}]^-$ ($R = H$,[1] F, Me,[1] Et,[2,3] Bz[3])[4] and $[1\text{-}H\text{–}CB_9F_9]^-$,[4] are among the weakest coordinating anions,[1,4,5] and many reactive electrophilic cations were stabilized in their presence, for example, $[Me_2Al]^+$,[6] $[Rh(CO)_4]^+$,[2] and $[Cu(CO)_4]^+$.[3] Fluorination of $[1\text{-}H\text{–}CB_{11}H_{11}]^-$ in anhydrous hydrogen fluoride (aHF) with elemental F_2 results in salts of the $[1\text{-}H\text{–}CB_{11}F_{11}]^-$ anion [eq (1)].[1,4]

$$Cs[1\text{-}H\text{-}CB_{11}H_{11}] + 11\ F_2 \xrightarrow[-78\ ^\circ C \rightarrow RT]{aHF} Cs[1\text{-}H\text{-}CB_{11}F_{11}] + 11\ HF \quad (1)$$

Deprotonation of $[1\text{-}H\text{–}CB_{11}F_{11}]^-$ with aqueous NaOH, followed by the addition of electrophiles, yields carborate anions with various nonfunctionalized substituents at the cluster carbon atom: $[1\text{-}R\text{-}CB_{11}F_{11}]^-$ ($R = F$, Me, Et, Bz).[1,4]

Incorporation of one or more functional groups into the periphery of the $[1\text{-}R\text{-}CB_{11}F_{11}]^-$ anion would result in building blocks with a fluorinated surface for ligand design with potential applications in the field of coordination polymers, crystal engineering, fluorous biphasic catalysis,[7,8] and ionic liquids.[9] Furthermore, such anions are of interest for the preparation of ionomers and pharmaceuticals.[9] A first example for a transition-metal complex with a fluorinated *closo*-carborate anion is the dianionic copper(I) complex $[1\text{-}ClCu\text{–}CB_{11}F_{11}]^{2-}$, which was obtained by the reaction of $[1\text{-}H\text{–}CB_{11}F_{11}]^-$ with $[Cu(mesityl)]_n$ in the presence of $[nBu_4N]Cl$ in dichloromethane.[1,4] The most-simple access to highly fluorinated *closo*-carborate anions with one functional group is the variation of the substituent R in $[1\text{-}R\text{-}CB_{11}F_{11}]^-$, either after fluorination of $[1\text{-}H\text{–}CB_{11}F_{11}]^-$ or before fluorination of $[1\text{-}H\text{–}CB_{11}H_{11}]^-$; although, so far, variation of the substituent was achieved after fluorination only.

In this contribution, we report on the fluorination of the $[1\text{-}H_2N\text{–}CB_{11}H_{11}]^-$ anion (**1**) to give the 1-aminoundecafluoro-1-carba-*closo*-dodecaborate anion $[1\text{-}H_2N\text{–}CB_{11}F_{11}]^-$

* To whom correspondence should be addressed. E-mail: maik.finze@uni-duesseldorf.de.
† Heinrich-Heine-Universität Düsseldorf.
‡ Universität Duisburg-Essen.

(1) Ivanov, S. V.; Rockwell, J. J.; Polyakov, O. G.; Gaudinski, C. M.; Anderson, O. P.; Solntsev, K. A.; Strauss, S. H. *J. Am. Chem. Soc.* **1998**, *120*, 4224.
(2) Lupinetti, A. J.; Havighurst, M. D.; Miller, S. M.; Anderson, O. P.; Strauss, S. H. *J. Am. Chem. Soc.* **1999**, *121*, 11920.
(3) Ivanova, S. M.; Ivanov, S. V.; Miller, S. M.; Anderson, O. P.; Solntsev, K. A.; Strauss, S. H. *Inorg. Chem.* **1999**, *38*, 3756.
(4) Strauss, S. H.; Ivanov, S. V.; Lupinetti, A. J. (Colorado State University Research Foundation). Patent WO 98/43983, 1998.
(5) Krossing, I.; Raabe, I. *Angew. Chem., Int. Ed.* **2004**, *43*, 2066.
(6) Strauss, S. H.; Ivanov, S. V. (Colorado State University Research Foundation). Patent WO 02/42367/A2, 2002.
(7) Horváth, I. T. *Acc. Chem. Res.* **1998**, *31*, 641.
(8) Dobbs, A. P.; Kimberley, M. R. *J. Fluorine Chem.* **2002**, *118*, 3.
(9) Kirsch, P. *Modern Fluoroorganic Chemsitry*; Wiley-VCH Verlag GmbH & Co.: Weinheim, Germany, 2004.

10.1021/ic701398u CCC: $37.00
Published on Web 10/19/2007

(**2**) and its reactions yielding the 1-aminodecafluoro-6-hydroxy-1-carba-*closo*-dodecaborate anion [1-H_2N-6-HO−$CB_{11}F_{10}$]$^-$ (**3**) and the 1-aminononafluoro-4,6-dihydroxy-1-carba-*closo*-dodecaborate anion [1-H_2N-4,6-$(HO)_2$−$CB_{11}F_9$]$^-$ (**4**), respectively. Only a few other halogenated derivatives of **1** or 1-ammonio-*closo*-carborane have been reported so far:[10] examples are [1-H_2N−$CB_{11}I_{11}$]$^-$,[11] [1-H_2N-7,8,9,10,-11,12-I_6−$CB_{11}H_5$]$^-$,[11] 12-I-1-R_3N−$CB_{11}H_{10}$ (R_3N = 4-pentylquinuclidin-1-yl),[12] and 1-Me_3N-12-Cl−$CB_{11}H_{10}$.[13] In contrast to **1**, for the related 1-aminocarba-*closo*-decaborate anion, the perchlorinated, perbrominated and periodinated species [1-H_2N−CB_9Hal_9]$^-$ (Hal = Cl, Br, I) were described;[14] to our knowledge, salts of the [1-H_2N−CB_9F_9]$^-$ anion are unknown, so far.

In addition to a description of the syntheses of salts of [1-H_2N−$CB_{11}F_{11}$]$^-$ (**2**), [1-H_2N-6-HO−$CB_{11}F_{10}$]$^-$ (**3**), and [1-H_2N-4,6-$(HO)_2$−$CB_{11}F_9$]$^-$ (**4**), thermal stabilities of these compounds are discussed, and they are characterized by vibrational and multi-NMR spectroscopy, as well as by mass spectrometry. Crystal structures are presented for some of the salts obtained. The spectroscopic and structural data are supported by values derived from DFT calculations.

Experimental Section

General Procedures and Reagents. Apparatus. Reactions involving air-sensitive compounds were performed under argon using standard Schlenk techniques. Fluorine and anhydrous hydrogen fluoride were manipulated in stainless-steel lines of known volume equipped with capacitance pressure gauges (type 280E Setra Instruments, Acton, MA) and with bellow valves (type BPV25004 Balzers and type SS4BG Nupro), as well as with Gyrolok and Cajon fittings. Fluorination reactions in anhydrous HF were performed in 100 or 250 mL reactors consisting of a PFA bulb with a NS29 socket standard taper (Bohlender, Lauda, Germany) in connection with a PFA NS29 cone standard taper and a PFA needle valve (type 204−30 Galtek, fluoroware, Chaska, MN). The parts were held together with a metal compression flange.

^{1}H, ^{11}B, ^{13}C, and ^{19}F NMR spectra were recorded at room temperature, either in D_2O or in CD_3CN on Bruker Avance DRX-500 spectrometers operating at 500.13, 125.76, 470.59, or 160.46 MHz for ^{1}H, ^{13}C, ^{19}F, and ^{11}B nuclei, respectively. NMR signals were referenced against TMS (^{1}H, ^{13}C), $CFCl_3$ (^{19}F), and BF_3·OEt_2 in CD_3CN (^{11}B) as external standards. Infrared and Raman spectra were recorded at room temperature on an Excalibur FTS 3500 spectrometer (Digilab, Germany) with an apodized resolution of 2 (IR) and 4 cm^{-1} (Raman), respectively. IR spectra were measured in the attenuated total reflection mode in the region of 4000−530 cm^{-1}. Raman spectra were measured using the 1064 nm excitation line of a Nd/YAG laser on crystalline samples contained in melting-point capillaries in the region of 3500−80 cm^{-1}. Matrix-assisted laser desorption/ionization (MALDI) mass spectra in the negative-ion mode were recorded on a Bruker Ultraflex TOF spectrometer. Thermoanalytical measurements were made with a Mettler Toledo DSC 30 instrument. Temperature and sensitivity calibrations in the temperature range of 25−600 °C were carried out on samples of gallium, indium, lead, tin, and zinc. About 5−10 mg of the solid samples were weighed and contained in sealed aluminum crucibles, and the studies were performed with a heating rate of 5 K min^{-1}; throughout this process, the furnace was flushed with dry nitrogen. Phase transitions assigned to melting points were verified visually.

Chemicals. All of the standard chemicals were obtained from commercial sources. Solvents were dried and stored in flasks equipped with valves with PTFE stems (Young, London) over molecular sieves (4 Å) under an argon atmosphere. K[1-H_2N−$CB_{11}H_{11}$] (K$^+$**1**)[15] was prepared via 7-H_3N-*nido*-7-$CB_{10}H_{12}$ from $B_{10}H_{14}$, according to published procedures.[16] Decaborane(14) was obtained from Katchem s.r.o. (Praha, Czech Republic) or synthesized from Na[BH_4] and BF_3·OEt_2.[17] Anhydrous HF and fluorine were gifts from Solvay AG (Hannover, Germany) and were used as received.

Single-Crystal X-ray Diffraction. Crystals of [BzPh$_3$P]$^+$**1**, [BzPh$_3$P]$^+$**2**, [Ph$_4$P]$^+$**3**, and [Ph$_4$P]$^+$**4** suitable for X-ray diffraction were grown from CH_2Cl_2 solutions by slow uptake of pentane vapor. K$^+$**2** was crystallized from Et_2O solution by slow diffusion of CH_2Cl_2. The crystals were investigated with a Stoe IPDS diffractometer with the exception of K$^+$**2**, which was studied using a Stoe STADI CCD diffractometer using Mo Kα radiation (λ = 0.71073 Å) in all cases. Structures were solved by direct methods,[18] and refinement is based on full-matrix least-squares calculations on F^2.[19] All of the salts crystallize in the triclinic space group $P\bar{1}$ except for [Ph$_4$P]$^+$**3**, which crystallizes in the tetragonal space group $P4_2/n$. The positions of most of the hydrogen atoms were located via ΔF syntheses. Anisotropic displacement parameters were applied to all of the atoms heavier than hydrogen. For CH and CH_2 idealized bond lengths and angles were used. The isotropic displacement parameters of all of these hydrogen atoms were kept equal to 130% of the equivalent isotropic displacement parameters of the parent secondary and aromatic carbon atoms. Similarly, the hydrogen atoms of the amino group in the *closo*-carborate anions were refined using distance restraints, and their isotropic displacement parameters were kept equal to 150% of the equivalent isotropic displacement parameters of the respective parent nitrogen atom. The only exceptions are the structure of [PPh$_4$]$^+$**4**, where the positions of the hydrogen atoms of the amino substituents in both independent anions are refined without any restraints, and the isotropic displacement parameters for the hydrogen atoms are kept equal for each independent amino group and the structure [Ph$_4$P]$^+$**3** where calculated positions were used for the hydrogen atoms. The position of the hydrogen atom of the hydroxy group in [Ph$_4$P]$^+$**3** was calculated as well. The hydrogen atoms of the two hydroxide groups in [PPh$_4$]$^+$**4**, which are involved in hydrogen bonding to an amino substituent, are treated analogously to the amino hydrogen atoms. In contrast, the other hydrogen atoms of the remaining two OH groups are refined via distant restraints, and their isotropic displacement parameters were kept equal to 150% of the equivalent isotropic displacement parameters of the respective parent oxygen atom. The hydrogen atoms bonded to boron in the structure of

(10) Körbe, S.; Schreiber, P. J.; Michl, J. *Chem. Rev.* **2006**, *106*, 5208.
(11) Srivastava, R. R.; Hamlin, D. K.; Wilbur, D. S. *J. Org. Chem.* **1996**, *61*, 9041.
(12) Douglass, A. G.; Janousek, Z.; Kaszynski, P. *Inorg. Chem.* **1998**, *37*, 6361.
(13) Khan, S. A.; Morris, J. H.; Siddiqui, S. *J. Chem. Soc., Dalton Trans.* **1990**, 2053.
(14) Tsang, C.-W.; Yang, Q.; Sze, E. T.-P.; Mak, T. C. W.; Chan, D. T. W.; Xie, Z. *Inorg. Chem.* **2000**, *39*, 3582.
(15) Jelínek, T.; Plešek, J.; Heřmánek, S.; Štíbr, B. *Collect. Czech. Chem. Commun.* **1986**, *51*, 819.
(16) Plešek, J.; Jelínek, T.; Drdakova, E.; Heřmánek, S.; Štíbr, B. *Collect. Czech. Chem. Commun.* **1984**, *49*, 1559.
(17) Dunks, G. B.; Barker, K.; Hedaya, E.; Hefner, C.; Palmerordonez, K.; Remec, P. *Inorg. Chem.* **1981**, *20*, 1692.
(18) Sheldrick, G. M. *SHELXS-97, Program for Crystal Structure Solution*; Universität Göttingen: Göttingen, Germany, 1997.
(19) Sheldrick, G. M. *SHELXL-97, Program for Crystal Structure Refinement*; Universität Göttingen: Göttingen, Germany, 1997.

Table 1. Crystallographic Data of M[1-$H_2N-CB_{11}F_{11}$] (M^+**2**, M = [$BzPh_3P$], K), [$BzPh_3P$][1-$H_2N-CB_{11}H_{11}$] ([$BzPh_3P$]$^+$**1**), [Ph_4P][1-H_2N-6-HO$-CB_{11}F_{10}$] ([Ph_4P]$^+$**3**), and [Ph_4P][1-H_2N-4,6-$(HO)_2-CB_{11}F_9$] ([Ph_4P]$^+$**4**)

compound	K^+**2**	[$BzPh_3P$]$^+$**2**	[$BzPh_3P$]$^+$**1**	[Ph_4P]$^+$**3**	[Ph_4P]$^+$**4**
empirical formula	$CH_2B_{11}F_{11}KN$	$C_{26}H_{24}B_{11}F_{11}NP$	$C_{26}H_{35}B_{11}NP$	$C_{25}H_{23}B_{11}F_{10}NOP$	$C_{25}H_{24}B_{11}F_9NO_2P$
fw (g mol^{-1})	395.031	709.357	511.467	693.339	691.348
color	colorless	colorless	colorless	colorless	colorless
cryst syst, space group	triclinic, $P\bar{1}$ (no. 2)	triclinic, $P\bar{1}$ (no. 2)	triclinic, $P\bar{1}$ (no. 2)	tetragonal, $P4_2/n$ (no. 86)	triclinic, $P\bar{1}$ (no. 2)
a (Å)	7.213(6)	13.941(3)	11.395(2)	14.286(2)	14.645(3)
b (Å)	7.730(7)	16.153(3)	11.420(2)		16.044(3)
c (Å)	13.057(9)	21.705(4)	12.667(3)	14.803(3)	16.268(3)
α (deg)	74.04(7)	75.40(3)	111.26(3)		97.96(3)
β (deg)	73.02(7)	85.84(3)	102.71(3)		111.13(3)
γ (deg)	66.71(8)	81.25(3)	96.08(3)		115.81(3)
V (Å^3)	628.9(9)	4671.7(16)	1466.8(5)	3020.9(9)	3004.3(10)
Z	2	6	2	4	4
ρ_{calcd} (Mg m^{-3})	2.086	1.513	1.158	1.522	1.528
μ (mm^{-1})	0.547	0.178	0.112	0.179	0.178
F(000) (e)	376	2136	536	1388	1392
θ range (deg)	4.97−24.49	3.75−25.00	4.09−24.99	4.21−25.00	4.21−25.00
R1 [$I > 2\sigma(I)$] (%)[a]	7.97	3.94	5.11	4.46	4.36
wR2 (all data) (%)[b]	18.86	7.51	9.96	9.13	8.93
GOF on F^2[c]	1.034	1.010	1.036	1.091	1.028

[a] $R1 = (\sum||F_o| - |F_c||)/\sum|F_o|$. [b] $wR2 = [\sum w(F_o^2 - F_c^2)^2/\sum w(F_o^2)^2]^{0.5}$, weight scheme: $w = [\sigma^2F_o + (aP)^2 + bP]^{-1}$; $P = [\max(0,F_o^2) + 2F_c^2]/3$; K^+**2**: $a = 0.01$, $b = 8.0$; [$BzPh_3P$]$^+$**2**: $a = 0.01$, $b = 0.5$; [$BzPh_3P$]$^+$**1**: $a = 0.02$, $b = 0.5$; [Ph_4P]$^+$**3**: $a = 0.025$, $b = 0.5$; [Ph_4P]$^+$**4**: $a = 0.02$, $b = 0.5$. [c] GOF $S = \sum w(F_o^2 - F_c^2)^2/(m - n)$; ($m$ = reflections, n = variables).

[$BzPh_3P$]$^+$**1**, were refined via distant restraints, and their isotropic displacement parameters were kept equal to 150% of the equivalent isotropic displacement parameters of the respective parent boron atom.

The carbon and nitrogen atoms in the two crystallographically independent anions in the structure of K^+**2** are disordered over all 12 possible positions; hence, structure refinement was performed with an occupancy of $^1/_{12}$ for carbon and nitrogen and $^{11}/_{12}$ for boron and fluorine, respectively.

Similar to **1** in its potassium salt, in the solid-state structure of [PPh_4]$^+$**3**, the anion is strongly disordered. The 12 positions in the *closo*-cluster are shared by 1 carbon and 11 boron atoms, and all 12 exohedral positions are refined with an occupancy of $^1/_{12}$ for oxygen as well as for nitrogen and $^{10}/_{12}$ for fluorine.

In the solid-state structure of [$BzPh_3P$]$^+$**1**, the $C-NH_2$ fragment is disordered over two positions: occupation 0.57(1)/0.43(1).

Molecular structure diagrams were drawn with the program *Diamond*.[20] Experimental details and crystal data were collected in Table 1. CCDC-653915 [$BzPh_3P$]$^+$**1**, CCDC-653916 K^+**2**, CCDC-653914 [$BzPh_3P$]$^+$**2**, CCDC-653917 [PPh_4]$^+$**3**, and CCDC-653918 [PPh_4]$^+$**4** contain the supplementary crystallographic data for this article. These data are deposited in the Supporting Material or can be obtained free of charge from the Cambridge Crystallographic Data Centre via www.ccdc.cam.ac.uk/data_request/cif.

Quantum Chemical Calculations. DFT calculations[21] were carried out using Becke's three-parameter hybrid functional and the Lee−Yang−Parr correlation functional (B3LYP)[22−24] with the *Gaussian 03* program suite.[25] Geometries were optimized, and energies were calculated with the 6-311++G(d,p) basis set. All of the structures represent true minima on the respective hypersurface (no imaginary frequency). Diffuse functions were incorporated because improved energies are obtained for anions.[26] DFT-GIAO[27] NMR shielding constants $\sigma(^{11}B)$, $\sigma(^{13}C)$, and $\sigma(^{19}F)$ were calculated at the B3LYP/6-311++G(2d,p) level of theory. The ^{11}B, ^{13}C, and ^{19}F NMR shielding constants were calibrated to the respective chemical shift scale $\delta(^{11}B)$, $\delta(^{13}C)$, and $\delta(^{19}F)$ using predictions on diborane(6), Me_4Si, and $CFCl_3$ with chemical shifts of −16.6 ppm for B_2H_6[28] and 0 ppm for Me_4Si, as well as for $CFCl_3$.[29]

Synthetic Reactions. K[1-$H_2N-CB_{11}F_{11}$] (K^+2). A 250 mL PFA reactor equipped with a magnetic stirring bar was charged with K^+**1** (1.72 g, 8.7 mmol) and 20 mL of anhydrous HF. Elemental fluorine (65 mmol) was carefully added to the white suspension over a period of 10 h at −78 °C. The reaction mixture was allowed to warm to room temperature overnight. The suspension was recooled to −78 °C, and fluorine was added (19 mmol). Subsequently, the reaction mixture was warmed to room temperature in 1 h and stirred for at least 4 additional hours. This procedure was repeated 4 times, and after the last addition, the suspension was kept at room temperature for 3 d to ensure completion of the reaction. The residual fluorine was removed under reduced pressure at −78 °C. After the removal of HF, a white solid remained in the reactor. The residue was extracted with three portions of diethyl

(20) Brandenburg, K. *Diamond, Version 3.1b*; Crystal Impact GbR: Bonn, Germany, 2006.
(21) Kohn, W.; Sham, L. J. *Phys. Rev. A* **1965**, *140*, 1133.
(22) Becke, A. D. *Phys. Rev. B: Condens. Matter* **1988**, *38*, 3098.
(23) Becke, A. D. *J. Chem. Phys.* **1993**, *98*, 5648.
(24) Lee, C.; Yang, W.; Parr, R. G. *Phys. Rev. B: Condens. Matter* **1988**, *41*, 785.
(25) Frisch, M. J.; Trucks, G. W.; Schlegel, H. B.; Scuseria, G. E.; Robb, M. A.; Cheeseman, J. R.; Montgomery, J. A., Jr.; Vreven, T.; Kudin, K. N.; Burant, J. C.; Millam, J. M.; Iyengar, S. S.; Tomasi, J.; Barone, V.; Mennucci, B.; Cossi, M.; Scalmani, G.; Rega, N.; Petersson, G. A.; Nakatsuji, H.; Hada, M.; Ehara, M.; Toyota, K.; Fukuda, R.; Hasegawa, J.; Ishida, M.; Nakajima, T.; Honda, Y.; Kitao, O.; Nakai, H.; Klene, M.; Li, X.; Knox, J. E.; Hratchian, H. P.; Cross, J. B.; Bakken, V.; Adamo, C.; Jaramillo, J.; Gomperts, R.; Stratmann, R. E.; Yazyev, O.; Austin, A. J.; Cammi, R.; Pomelli, C.; Ochterski, J. W.; Ayala, P. Y.; Morokuma, K.; Voth, G. A.; Salvador, P.; Dannenberg, J. J.; Zakrzewski, V. G.; Dapprich, S.; Daniels, A. D.; Strain, M. C.; Farkas, O.; Malick, D. K.; Rabuck, A. D.; Raghavachari, K.; Foresman, J. B.; Ortiz, J. V.; Cui, Q.; Baboul, A. G.; Clifford, S.; Cioslowski, J.; Stefanov, B. B.; Liu, G.; Liashenko, A.; Piskorz, P.; Komaromi, I.; Martin, R. L.; Fox, D. J.; Keith, T.; Al-Laham, M. A.; Peng, C. Y.; Nanayakkara, A.; Challacombe, M.; Gill, P. M. W.; Johnson, B.; Chen, W.; Wong, M. W.; Gonzalez, C.; Pople, J. A. *Gaussian 03*, revision C.02; Gaussian, Inc.: Wallingford, CT, 2004.
(26) Rienstra-Kiracofe, J. C.; Tschumper, G. S.; Schaefer, H. F., III.; Nandi, S.; Ellison, G. B. *Chem. Rev.* **2002**, *102*, 231.
(27) Wolinski, K.; Hinton, J. F.; Pulay, P. *J. Am. Chem. Soc.* **1990**, *112*, 8251.
(28) Kennedy, J. D., Boron. In *Multinuclear NMR*; Mason, J., Ed.; Plenum Press: New York, 1987; p 221.
(29) Berger, S.; Braun, S.; Kalinowski, H.-O. *NMR-Spektroskopie von Nichtmetallen - ^{19}F-NMR-Spektroskopie*, 4th ed.; Georg Thieme Verlag: Stuttgart, Germany, 1994.

ether (100 mL, 50 mL, 50 mL). The ether was removed under vacuum, and colorless K^+**2** was obtained. Yield: 1.67 g (4.2 mmol, 49%): MS(MALDI): *m*/*z* (isotopic abundance): Calcd for **2**: 350(<1), 351(1), 352(3), 353(13), 354(37), 355(74), 356(100), 357(81), 358(30), 359(<1); Found: 350(0), 351(<1), 352(1), 353(7), 354(39), 355(78), 356(100), 357(86), 358(28), 359(<1).

K[1-H_2N-$^{13}CB_{11}F_{11}$]. The ^{13}C-labeled compound was synthesized as described for the nonlabeled substance.

[$BzPh_3P$][1-H_2N−$CB_{11}F_{11}$] ([$BzPh_3P$]$^+$2). A solution of [$BzPh_3P$]Br (1 g, 2.3 mmol) in 50 mL of water was added dropwise to a solution of K^+**2** (230 mg, 0.58 mmol) in 25 mL of water, and immediately white [$BzPh_3P$]$^+$**2** precipitated. The solid was separated by filtration and dried in a vacuum. Yield 376 mg (0.53 mmol, 91%).

[$BzPh_3P$][1-H_2N−$CB_{11}H_{11}$] ([$BzPh_3P$]$^+$1). White [$BzPh_3P$]$^+$**1** precipitated from a solution of K^+**1** (370 mg, 1.9 mmol) in 30 mL of water upon the addition of an aqueous solution of [$BzPh_3P$]Br (2 g, 4.6 mmol, 120 mL). Yield: 869 mg (1.7 mmol, 89%); MS(MALDI): *m*/*z* (isotopic abundance): Calcd for **1**: 152(<1), 153(1), 154(3), 155(13), 156(37), 157(74), 158(100), 159(81), 160(30), 161(<1); Found: 152(0), 153(<1), 154(2), 155(10), 156(42), 157(75), 158(100), 159(88), 160(29), 161(<1).

[Ph_4P][1-H_2N-6-HO−$CB_{11}F_{10}$] ([Ph_4P]$^+$3). K^+**2** (53 mg, 0.13 mmol) was added to a solution of KOH (1 g, 18 mmol) in 5 mL of water, and after 20 min, all of the solid dissolved. The reaction mixture was stirred for a further 10 min and then added to an aqueous solution of $NaHCO_3$ (5 mL) while stirring. The resulting clear reaction mixture was immediately added to a stirred solution of [Ph_4P]Br (500 mg, 1.2 mmol) in 25 mL of water, resulting in the formation of a white precipitate: [Ph_4P]$^+$**3**, which was isolated via filtration and dried in a vacuum. Yield: 70 mg (0.10 mmol, 77%); MS(MALDI): *m*/*z* (isotopic abundance): Calcd for **3**: 348(<1), 349(1), 350(3), 351(13), 352(37), 353(74), 354(100), 355(81), 356(31), 357(1), 358(<1); Found: 348(0), 349(1), 350(3), 351(14), 352(40), 353(82), 354(100), 355(87), 356(34), 357(0), 358(0).

[Ph4P][4,6-$(HO)_2$-1-H_2N−$CB_{11}F_9$] ([Ph_4P]$^+$4). Solid K^+**2** (90 mg, 0.23 mmol) was added to KOH (1.2 g, 21 mmol) dissolved in 6 mL of water. The reaction mixture was stirred for 4 d. The clear colorless solution was poured into a solution of $NaHCO_3$ in 5 mL of water, and, subsequently, this mixture was added dropwise to a solution of [Ph_4P]Br (900 mg, 2.1 mmol) in 50 mL of water. Immediately, white [Ph_4P]$^+$**4** precipitated from the mixture. The product was separated by filtration and dried under reduced pressure. Yield: 118 mg (0.17 mmol, 74%): MS(MALDI): *m*/*z* (isotopic abundance): Calcd for **4**: 346(<1), 347(1), 348(3), 349(13), 350(37), 351(74), 352(100), 353(81), 354(31), 355(1), 356(<1); Found: 346(0), 347(<1), 348(7), 349(27), 350(65), 351(78), 352(100), 353(80), 354(50), 355(1), 356(0).

Results and Discussion

Synthetic Aspects. The potassium salt of the [1-H_2N−$CB_{11}H_{11}$]$^-$ anion (**1**) was fluorinated in anhydrous HF with elemental fluorine to produce K[1-H_2N−$CB_{11}F_{11}$] (K^+**2**) in a yield of 49% according to eq 2.

$$K[1\text{-}H_2N\text{-}CB_{11}H_{11}] + 11\ F_2 \xrightarrow[-78\ ^\circ C \rightarrow RT]{aHF} K[1\text{-}H_2N\text{-}CB_{11}F_{11}] + 11\ HF \quad (2)$$

This synthesis parallels the preparation of salts of the [1-H−$CB_{11}F_{11}$]$^-$ anion starting from Cs[1-H−$CB_{11}H_{11}$] [eq (1)].[1,4] Varying small amounts of salts of [1-H_2N−CB_{11}-HF_{10}]$^-$ (Figure S1 in the Supporting Information), and for some reactions, smaller amounts of [1-H_2N−$CB_{11}H_2F_9$]$^-$ were detected by mass spectrometry. The position of the hydrogen atom in [1-H_2N-6-H−$CB_{11}F_{10}$]$^-$ was unambiguously assigned by NMR spectroscopy, whereas the NMR data indicate a mixture of at least two isomers for the [1-H_2N−$CB_{11}H_2F_9$]$^-$ anion: most likely [1-H_2N-4,6-H_2−$CB_{11}F_9$]$^-$ and [1-H_2N-5,6-H_2−$CB_{11}F_9$]$^-$. Other side products formed are the borate anions [BF_3CN]$^-$ and [BF_4]$^-$ as a result of cluster degradation. The formation of the [BF_3CN]$^-$ anion[30] is proven by ^{11}B, ^{19}F, and ^{13}C NMR spectroscopy from a fluorination experiment with isotopically labeled **1**. Its unprecedented formation is explained by transformation of the C−NH_2 fragment in **1** into a cyano group.

Attempted selective fluorination of **1** to produce [1-H_2N-7,8,9,10,11,12-F_6−$CB_{11}H_5$]$^-$ by using 6 equiv of fluorine failed, and a mixture of 1-amino-*closo*-carborate anions with up to nine fluorine atoms attached to boron was obtained. Although synthetic details on the preparation of salts of related anion [1-H-7,8,9,10,11,12-F_6−$CB_{11}H_5$]$^-$ have not been reported so far, some spectroscopic and structural properties were published.[31]

Except for a probable protonation yielding 1-H_3N−$CB_{11}H_{11}$, a reaction of K^+**1** with anhydrous HF does not occur; a sample of the 1-amino-*closo*-carborate was kept for 3 days at 50 °C, without traces of fluorinated species being formed. This observation contrasts the findings in the case of the [1-H−$CB_{11}H_{11}$]$^-$ anion, which is regioselectively fluorinated with HF under the formation of hydrogen at 23 °C in 22 h to give the [1-H-12-F−$CB_{11}H_{10}$]$^-$ anion.[32] At higher temperatures, selective fluorination to [1-H-7,12-F_2−$CB_{11}H_9$]$^-$ and [1-H-7,9,12-F_6−$CB_{11}H_5$]$^-$ was achieved.[32] Under more severe conditions, a mixture of fluorinated *closo*-carborate anions [1-H−$CB_{11}H_{11-n}F_n$]$^-$ (n = 6−9) was obtained.[4] A similar inertness against anhydrous HF as found for K^+**1** was previously reported for the related *closo*-borate anion [H_3N−$B_{12}H_{11}$]$^-$, which was recovered from anhydrous HF after 2 days at 25 °C nearly quantitatively, and fluorinated species had formed in small amounts only.[6,33]

The potassium salt of K[1-H_2N−$CB_{11}F_{11}$] (K^+**2**) is an air-stable white solid that exhibits two reversible phase transitions at 65 and 238 °C, respectively, and it exothermically decomposes at 338 °C, according to DSC measurements. Hence, its thermal stability is reduced compared to the nonfluorinated salt K^+**1**, which undergoes a reversible endothermic phase transition at 142 °C and begins to decompose at 511 °C.

Decomposition of K^+**2** in water is slow, but after 1 day, signals of the anion are not present in the NMR spectra anymore. As a result of the complexity of these NMR spectra, an assignment of the signals is not possible. Immediate

(30) Bernhardt, E.; Berkei, M.; Willner, H.; Schürmann, M. *Z. Anorg. Allg. Chem.* **2003**, *629*, 677.
(31) McLemore, D. K.; Dixon, D. A.; Strauss, S. H. *Inorg. Chim. Acta* **1999**, *294*, 193.
(32) Ivanov, S. V.; Lupinetti, A. J.; Miller, S. M.; Anderson, O. P.; Solntsev, K. A.; Strauss, S. H. *Inorg. Chem.* **1995**, *34*, 6419.
(33) Ivanov, S. V.; Davis, J. A.; Miller, S. M.; Anderson, O. P.; Strauss, S. H. *Inorg. Chem.* **2003**, *42*, 4489.

Table 2. Selected Calculated[a] and Experimental Bond Lengths of the *closo*-Carborate Anions $[1\text{-}H_2N\text{-}4,6\text{-}(HO)_2\text{-}CB_{11}F_9]^-$ (**4**), $[1\text{-}H_2N\text{-}6\text{-}HO\text{-}CB_{11}F_{10}]^-$ (**3**), $[1\text{-}H_2N\text{-}CB_{11}F_{11}]^-$ (**2**), $[1\text{-}H_2N\text{-}CB_{11}H_{11}]^-$ (**1**), $[1\text{-}H\text{-}CB_{11}F_{11}]^-$, and $[1\text{-}H\text{-}CB_{11}H_{11}]^-$

	4		3	2		1	$[1\text{-}H\text{-}CB_{11}F_{11}]^-$	$[1\text{-}Et\text{-}CB_{11}F_{11}]^-$	$[1\text{-}H\text{-}CB_{11}H_{11}]^-$	
anion	calcd	$[Ph_4P]^+$ [b]	calcd	calcd	$[BzPh_3P]^+$ [b]	calcd	calcd	$[Cu(CO)_4]^+$ [3]	calcd	$[Ag(Ph_3P)_2]^+$ [54]
symmetry	C_s	C_1	C_1	C_s	C_1	C_s	C_{5v}	C_1	C_{5v}	C_1
C−N	1.472	1.443(4)	1.430	1.427	1.428(4)	1.451				
C−B	1.733	1.730(5)	1.733	1.734	1.720(5)	1.719	1.716	1.733(4)	1.707	1.728(5)
B2−B6[c]	1.795	1.802(7)	1.797	1.794	1.779(6)	1.765	1.797	1.790(4)	1.780	1.756(5)
B7−B11[c]	1.807	1.807(8)	1.814	1.814	1.803(6)	1.787	1.815	1.806(4)	1.789	1.781(4)
B2−B7[c]	1.780	1.781(6)	1.777	1.777	1.762(5)	1.772	1.779	1.778(4)	1.774	1.760(4)
B7−B12[c]	1.801	1.795(7)	1.803	1.803	1.787(6)	1.785	1.803	1.796(4)	1.786	1.776(4)
B2−F[c]	1.359	1.359(5)	1.369	1.365	1.354(4)		1.365	1.353(3)		
B−O[c]	1.405	1.378(5)	1.394							
B7−F[c]	1.377	1.368(5)	1.373	1.373	1.364(5)		1.372	1.369(4)		
B12−F	1.374	1.374(4)	1.373	1.372	1.374(4)		1.372	1.375(3)		

[a] B3LYP/6-311++G(d,p). [b] This work. [c] Mean values.

addition of aqueous solutions of salts of weakly coordinating cations to freshly prepared solutions of K^+**2** in water give white precipitates of the corresponding salts with the *closo*-carborate anion. An example is $[BzPh_3P]^+$**2**, which is a white solid that melts at 204 °C and decomposes at 410 °C.

In concentrated aqueous KOH, the $[1\text{-}H_2N\text{-}CB_{11}F_{11}]^-$ anion (**1**) regioselectively reacts to give the $[1\text{-}H_2N\text{-}4,6\text{-}(HO)_2\text{-}CB_{11}F_9]^-$ anion (**4**) after 4 days via $[1\text{-}H_2N\text{-}6\text{-}HO\text{-}CB_{11}F_{10}]^-$ (**3**), which is formed as an intermediate in 20−30 min [eq (3) and (4)].

$$[1\text{-}H_2N\text{-}CB_{11}F_{11}]^- + OH^- \xrightarrow[\text{RT, 30 min}]{H_2O/KOH} [1\text{-}H_2N\text{-}6\text{-}HO\text{-}CB_{11}F_{11}]^- + F^- \quad (3)$$

$$[1\text{-}H_2N\text{-}CB_{11}F_{11}]^- + 2\ OH^- \xrightarrow[\text{RT, 4 d}]{H_2O/KOH} [1\text{-}H_2N\text{-}4,6\text{-}(HO)_2\text{-}CB_{11}F_{11}]^- + 2\ F^- \quad (4)$$

No further exchange of fluoride against hydroxide was observed, and the $[1\text{-}H_2N\text{-}4,6\text{-}(HO)_2\text{-}CB_{11}F_9]^-$ anion (**4**) − or more likely a deprotonated form thereof − is indefinitely stable in concentrated aqueous KOH. The only side products formed are small amounts (<10%) of $[B(OH)_4]^-$, as determined by ^{11}B NMR spectroscopy. The *closo*-carborate anions were isolated as white precipitates by adjusting the pH of the reaction mixtures to 7−8, followed by addition of an aqueous solution of $[Ph_4P]Br$. The MALDI mass spectra in the negative ion mode are depicted in Figure S2 in the Supporting Information. The salts melt at 276 °C ($[Ph_4P]^+$**4**) and 285 °C ($[Ph_4P]^+$**3**) and slowly start to decompose on further heating in the molten state (DSC measurements). The positions of the hydroxy substituents are in agreement with NMR spectroscopic data, and in the case of $[Ph_4P]^+$**4**, a crystal structure was obtained. Analogous reactions have been reported for the $[1\text{-}H\text{-}CB_{11}F_{11}]^-$ anion, resulting in $[1\text{-}H\text{-}CB_{11}F_{10}(OH)]^-$ and $[1\text{-}H\text{-}CB_{11}F_9(OH)_2]^-$.[1,4]

A remarkable difference of the related anions $[1\text{-}H_2N\text{-}CB_{11}F_{11}]^-$ (**2**) and $[1\text{-}H\text{-}CB_{11}F_{11}]^-$ is their stability toward acids: the amino substituted carborate anion rapidly decomposes in concentrated aqueous hydrochloric acid under gas evolution (t < 20 min); $[1\text{-}R\text{-}CB_{11}F_{11}]^-$ (R = H, Me) is indefinitely stable against 5 M hydrochloric and 5 M sulfuric acid.[1] A probable explanation for the instability of **2** against aqueous acids is the protonation of the amino group giving the electron poor inner salt $1\text{-}H_3N\text{-}CB_{11}F_{11}$, which is sensitive against the attack of water; so far, attempts have not been undertaken to protonate **2** in a different, more-inert solvent. Contrasting the behavior of **2**, the nonfluorinated *closo*-carborate anion $[1\text{-}H_2N\text{-}CB_{11}H_{11}]^-$ (**1**) is stable in concentrated acids, as well as in concentrated bases as shown by NMR spectroscopy. The isoelectronic borate anion $[1\text{-}H_3N\text{-}B_{12}F_{11}]^-$, as well as related $[1\text{-}Me_3N\text{-}B_{12}F_{11}]^-$, is stable against water also.[6,33] However, a comparable instability against water was reported for the neutral, highly fluorinated *closo*-carboranes *ortho*-$H_2C_2B_{10}F_{10}$, *meta*-$H_2C_2B_{10}F_{10}$,[34] *para*-$H_2C_2B_{10}F_{10}$, and *meta*-$C_2B_{10}F_{12}$.[35] In the series of decafluoro-*closo*-carboranes, the rate of hydrolysis increases in the order *para*-$H_2C_2B_{10}F_{10}$ < *meta*-$H_2C_2B_{10}F_{10}$ < *ortho*-$H_2C_2B_{10}F_{10}$.[35] Boric acid was reported to be the final product, and the formation of hydroxycarboranes as intermediates was assumed.

Structural Properties. The data of the crystal structures of K^+**2**, $[BzPh_3P]^+$**2**, $[BzPh_3P]^+$**1**, $[Ph_4P]^+$**3**, and $[Ph_4P]^+$**4** are summarized in Table 1. Because the aminocarba-*closo*-dodecaborate anions in the crystal structures of K^+**2**, $[BzPh_3P]^+$**1**, and $[Ph_4P]^+$**3** are disordered, a discussion of the bonding properties is arbitrary. Hence, selected bond parameters, derived from the diffraction studies on crystals of $[BzPh_3P]^+$**2** and $[Ph_4P]^+$**4**, are considered solely. These values are compared to values derived from DFT calculations and to parameters of selected related carborate clusters. In Table 2, averaged values are listed for related bond lengths because their deviations are very small; this is also the case for the B−B and B−F bonds of the upper (B2−B6) and lower (B7−B11) belts in **3** and **4**. Although a significant difference in bond length could be expected as a result of the influence of the hydroxy substituents in both anions; the deviations are small. In Figure 1, models of the calculated structures of $[1\text{-}H_2N\text{-}CB_{11}F_{11}]^-$ (**2**), $[1\text{-}H_2N\text{-}6\text{-}HO\text{-}CB_{11}F_{10}]^-$ (**3**), and $[1\text{-}H_2N\text{-}4,6\text{-}(HO)_2\text{-}CB_{11}F_9]^-$ (**4**) showing the labeling scheme are depicted.

The experimental and theoretical bond lengths in **2** and **4** are in very good agreement (Table 2, Figures 2and 3); hence, the calculated values for **3** probably also reflect the bonding

(34) Lagow, R. J.; Margrave, J. L. *J. Inorg. Nucl. Chem.* **1973**, *35*, 2085.
(35) Kongpricha, S.; Schroeder, H. *Inorg. Chem.* **1969**, *8*, 2449.

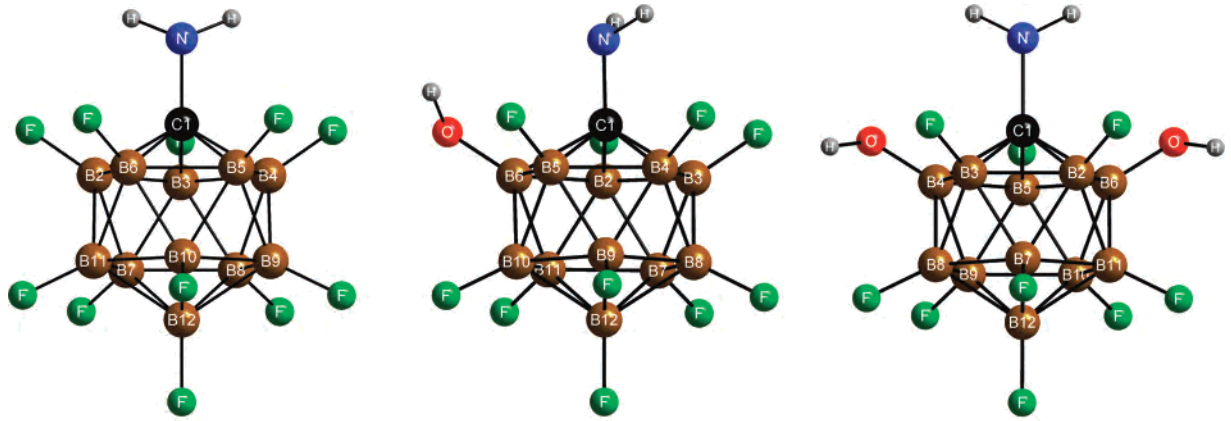

2 3 4

Figure 1. Representations of the calculated structures of the isoelectronic 1-aminocarba-*closo*-dodecaborate anions $[1\text{-}H_2N{-}CB_{11}F_{11}]^-$ (left), $[1\text{-}H_2N\text{-}6\text{-}HO{-}CB_{11}F_{10}]^-$ (middle), and $[1\text{-}H_2N\text{-}4,6\text{-}(HO)_2{-}CB_{11}F_9]^-$ (right).

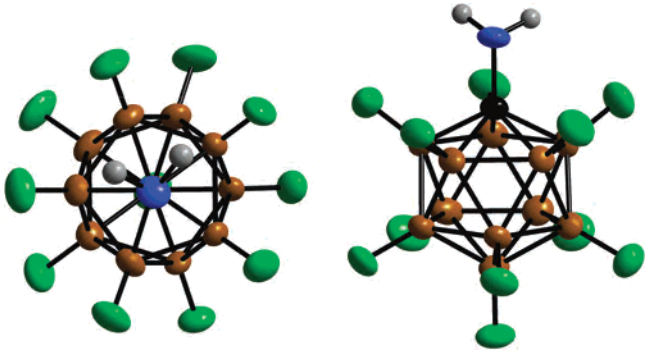

Figure 2. Model of one of the three independent $[1\text{-}H_2N{-}CB_{11}F_{11}]^-$ anions (**2**) in the solid-state structure of $[BzPh_3P]^+$**2** (50% probability ellipsoids except for hydrogens, which are depicted with arbitrary radii).

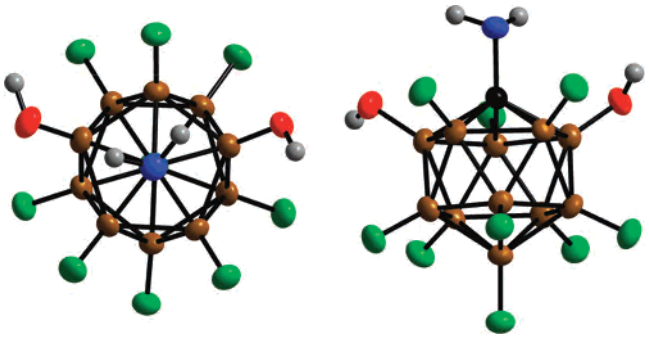

Figure 3. Model of one of the two independent $[1\text{-}H_2N\text{-}4,6\text{-}(HO)_2{-}CB_{11}F_9]^-$ anions (**4**) in the solid-state structure of $[Ph_4P]^+$**4** (50% probability ellipsoids except for hydrogens, which are depicted with arbitrary radii).

situation in the anion very well. The differences in the corresponding bond lengths in the series of the three isoelectronic aminocarba-*closo*-dodecaborate anions are very small − nearly all of the experimental differences are not significant ($<3\sigma$). A comparison of the theoretical values of **2**, which agree well with experimental numbers of the related $[1\text{-Et}{-}CB_{11}F_{11}]^-$ anion,[3] reveals similar small, negligible differences in bond lengths.

A comparison of the experimental and calculated C−B and B−B bond lengths of **2** to those of $[1\text{-}H_2N{-}CB_{11}H_{11}]^-$ (**1**) shows that all of the bonds in the fluorinated *closo*-carborate anion are elongated. A similar expansion of the cluster upon fluorination was described for $[1\text{-Et}{-}CB_{11}F_{11}]^-$/$[1\text{-Bz}{-}CB_{11}F_{11}]^-$ and $[1\text{-H}{-}CB_{11}H_{11}]^-$ previously[1,31] and reproduced by our calculations, too (Table 2). The reason is a removal of electron density from bonding orbitals of the cluster upon exchange of the hydrogen against fluorine substituents.[10,31]

In Figure 4, the hydrogen-bond system of the $[1\text{-}H_2N\text{-}4,6\text{-}(HO)_2{-}CB_{11}F_9]^-$ anions (**4**) in the solid state is depicted. A pair of anions forms a dimer with the inversion center located in their center. This hydrogen-bonded motif is formed via two hydrogen bonds with the hydroxy hydrogen atoms as donors and the amino nitrogen atoms as acceptors, and altogether it involves 10 atoms: $R^2_2(10)$.[36,37] The respective atomic distances (Figure 4) are in the range typical for O−H···N hydrogen bonds.[38] Related cyclic hydrogen-bonded motifs, $R^2_2(10)$, have been found for example in the solid-state structures of 1-hydroxy-2-aminobenzenes.[39,40]

The hydrogen atom of the second hydroxy group in the *closo*-carborate anions involved in the dimer also acts as a donor. The nitrogen atom of the second independent borate anion acts as hydrogen-bond acceptor. In contrast to both hydroxy groups of the first independent aminocarba-*closo*-dodecaborate anion, the two hydroxy groups of the second independent anion have only negligible interactions.

The closest distances between the weakly coordinating phosphonium cations and the respective 1-aminocarba-*closo*-dodecaborate anions are within the limits of weak interionic distances.[41]

NMR Spectroscopy. The fluorinated 1-aminocarba-*closo*-dodecaborate anions are characterized by multi-NMR spectroscopy, and the data are collected in Tables 3 and 4. The assignments of the ^{11}B and ^{19}F signals, listed in Table 3 and

(36) Etter, M. C.; MacDonald, J. C.; Bernstein, J. *Acta Crystallogr., Sect. B: Struct. Sci.* **1990**, *B46*, 256.
(37) Etter, M. C. *Acc. Chem. Res.* **1990**, *23*, 120.
(38) Hamilton, W. C.; Ibers, J. C. *Hydrogen Bonding in Solids*; W. A. Benjamin Inc.: New York, 1968.
(39) Blagden, N.; Cross, W. I.; Davey, R. J.; Broderick, M.; Pritchard, R. G.; Roberts, R. J.; Rowe, R. C. *Phys. Chem. Chem. Phys.* **2001**, *3*, 3819.
(40) Dey, A.; Kirchner, M. T.; Vangala, V. R.; Desiraju, G. R.; Mondal, R.; Howard, A. K. *J. Am. Chem. Soc.* **2005**, *127*, 10545.
(41) Shannon, R. D. *Acta Crystallogr., Sect. A: Found. Crystallogr.* **1976**, *32*, 751.

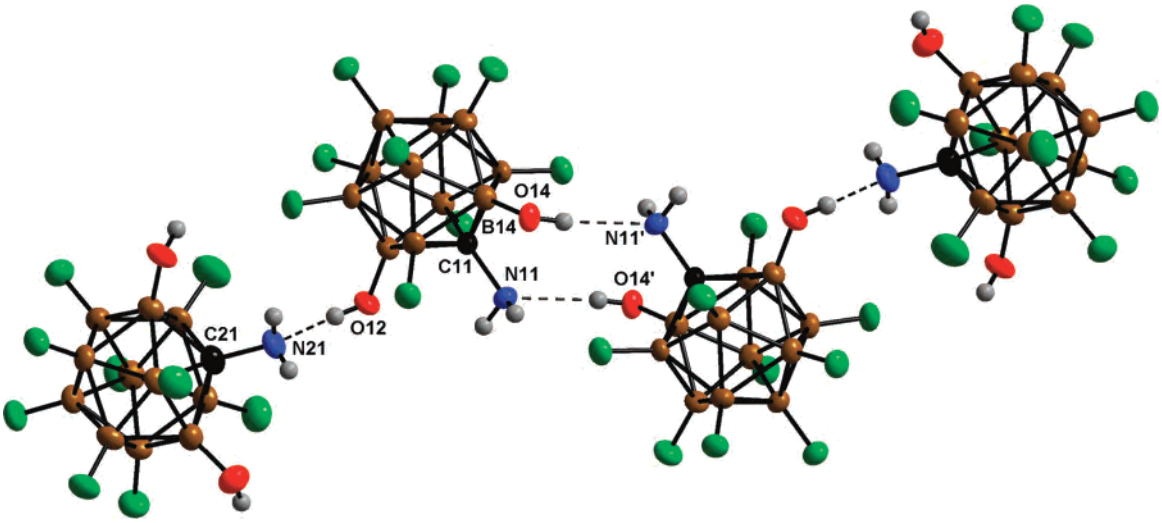

Figure 4. Hydrogen-bond system in the solid-state structure of $[Ph_4P]^+$**4** (50% probability ellipsoids except for hydrogens, which are depicted with arbitrary radii). Selected interatomic distances (Å) and angles (deg): O14···N11′, 2.921(4); N11′−H14, 2.13(6); O12···N21, 2.939(6); H12−N21, 2.10(7); O14−H14−N11′, 174(5); O12−H12−N21, 165(6).

Table 3. Experimental[a] and Calculated[b,c] ^{11}B and ^{19}F NMR Spectroscopic Data of $[1\text{-}H_2N{-}CB_{11}F_{11}]^-$ (**2**) and Related Carborate Anions

$\delta(^{11}B)_{exptl}$ [ppm]	$\delta\ (^{11}B)_{calcd}$ [ppm]	Δ^d [ppm]	$\delta\ (^{19}F)_{exptl}$ [ppm]	$\delta\ (^{19}F)_{calcd}$ [ppm]	Δ^e [ppm]	$^1J(^{11}B,^{19}F)_{exptl}$ [Hz]	assignment
$[1\text{-}H_2N{-}CB_{11}F_{11}]^-$ (**2**)							
−18.5	−20.0	−1.5	−255.9	−290.9	−35.0	44	2−6
−17.3	−18.3	−1.0	−263.3	−295.9	−32.6	42	7−11
−10.7	−11.8	−1.1	−252.7	−281.0	−28.3	59	12
$[1\text{-}H_2N\text{-}6\text{-}H{-}CB_{11}F_{10}]^-$							
n.o.[f]	−19.1		−255.4	−291.0	−35.6	51	2, 5
n.o.[f]	−18.1		−247.0	−279.6	−32.6	44	3, 4
−36.0	−35.9	0.1					6
−16.2	−17.0	−0.8	−254.1	−286.7	−32.6	42	7, 9
−13.7	−14.7	−1.0	−258.1	−290.7	−32.6	58	8
−14.4	−15.5	−1.1	−261.9	−294.6	−32.7	45	10, 11
−8.4	−8.5	−0.1	−240.3	−268.1	−27.8	61	12
$[1\text{-}H_2N\text{-}6\text{-}HO{-}CB_{11}F_{10}]^-$ (**3**)							
−18.1	−20.2	−2.1	−255.8	−292.8	−37.0	42	2, 5
−18.1	−20.3	−2.2	−254.9	−291.2	−36.3	43	3, 4
−19.7	−22.0	−2.3					6
−17.3	−18.4	−1.1	−263.1	−295.4	−32.3	47	7, 9
−18.1	−18.5	−0.4	−265.0	−297.0	−32.0	42	8
−16.7	−17.7	−1.0	−262.2	−294.8	−32.6	46	10, 11
−10.4	−10.6	−0.2	−251.9	−280.0	−28.1	59	12
$[1\text{-}H_2N\text{-}4,6\text{-}(HO)_2{-}CB_{11}F_9]^-$ (**4**)							
−17.7	−19.4	−1.7	−254.8	−290.7	−35.9	42	2, 3
−19.8	−22.4	−2.6					4, 6
−17.7	−19.5	−1.8	−254.0	−292.9	−38.9	42	5
−17.3	−18.1	−0.8	−262.9	−296.1	−32.2	41	7
−17.0	−17.9	−0.9	−263.8	−299.2	−35.4	42	8, 11
−16.6	−17.2	−0.6	−262.0	−295.2	−33.2	44	9, 10
−10.2	−11.3	−1.1	−251.1	−279.4	−28.3	60	12
$[1\text{-}H_2N{-}CB_{11}H_{11}]^-$ (**1**)[g, 15]							
−12.8	−14.9	−2.1					2−6
−14.5	−16.2	−1.7					7−11
−14.5	−15.6	−1.1					12
$[1\text{-}H{-}CB_{11}F_{11}]^-$ [g, 1]							
−18.2	−19.9	−1.7	−257.2	−291.6	−34.4	45	2−6
−16.6	−17.7	−1.1	−256.7	−289.1	−32.4	42	7−11
−8.5	−9.4	−0.9	−253.1	−282.0	−28.9	61	12
$[1\text{-}H{-}CB_{11}H_{11}]^-$ [g, 16]							
−16.2	−19.1	−2.9					2−6
−13.2	−15.1	−1.9					7−11
−6.8	−7.9	−1.1					12

[a] NMR solvent: CD_3CN. [b] Calculated with the GIAO method at the B3LYP/6-311++G(2d,p) level of theory using geometries at the B3LYP/6-311++G(d,p) level. [c] Values are averaged according to the highest possible local geometry of the respective cluster. [d] $\Delta = \delta(^{11}B)_{calcd} - \delta(^{11}B)_{exptl}$. [e] $\Delta = \delta(^{19}F)_{calcd} - \delta(^{19}F)_{exptl}$. [f] n.o. = not observed; NMR signals are covered by those of **2**. [g] This work.

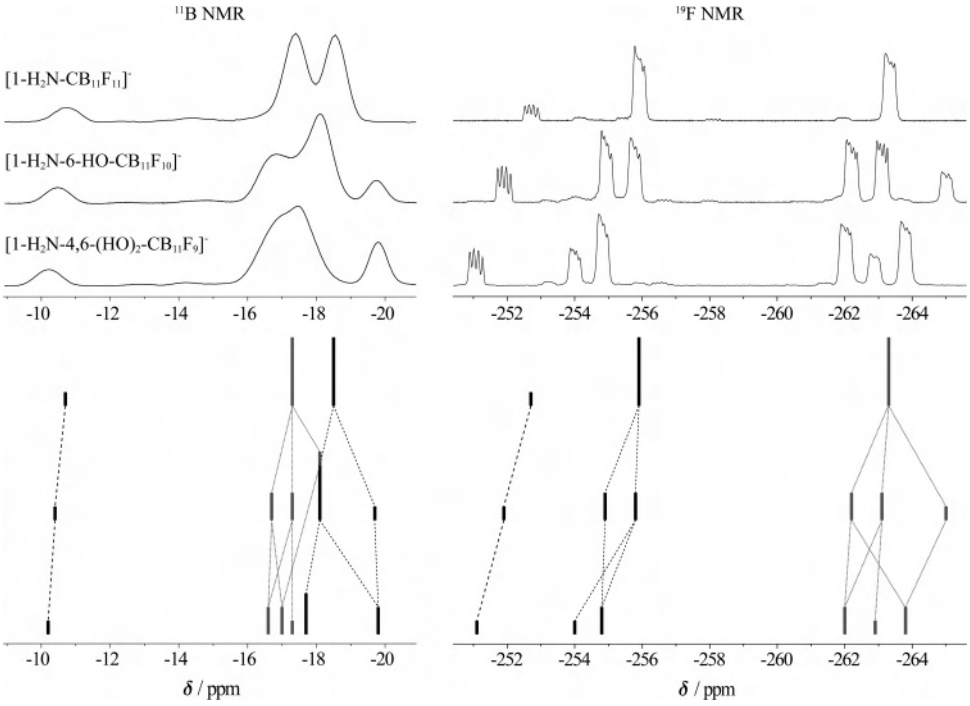

Figure 5. ^{11}B and ^{19}F NMR spectra (top) as well as stick diagrams showing the correlation between the signals (bottom) of the anions [1-H$_2$N−CB$_{11}$F$_{11}$]$^-$ (**2**), [1-H$_2$N-6-HO−CB$_{11}$F$_{11}$]$^-$ (**3**), and [1-H$_2$N-4,6-(HO)$_2$−CB$_{11}$F$_{11}$]$^-$ (**4**).

Table 4. Experimental[a] and Calculated[b] ^{13}C NMR Spectroscopic Data of [1-H$_2$N−CB$_{11}$F$_{11}$]$^-$ (**2**) and Related Carborate Anions

anion	$\delta(^{13}C)_{exptl}$ [ppm]	$\delta(^{13}C)_{calcd}$ [ppm]	Δ^c [ppm]
[1-H$_2$N−CB$_{11}$F$_{11}$]$^-$ (**2**)	37.0	40.5	3.5
[1-H$_2$N-6-H−CB$_{11}$F$_{10}$]$^-$	38.2	41.8	3.6
[1-H$_2$N−CB$_{11}$H$_{11}$]$^-$ (**1**)[d]	82.9	86.6	3.7
[1-H−CB$_{11}$F$_{11}$]$^-$ [e]	15.8	21.3	5.5
[1-H−CB$_{11}$H$_{11}$]$^-$ [f]	51.4	54.3	2.9

[a] NMR solvent: CD_3CN. [b] Calculated with the GIAO method at the B3LYP/6-311++G(2d,p) level of theory using geometries at the B3LYP/6-311++G(d,p) level. [c] $\Delta = \delta(^{13}C)_{calcd} - \delta(^{13}C)_{exptl}$. [d] This work. [e] NMR solvent: $(CD_3)_2CO$.[4] [f] No solvent specified.[10]

visualized in stick diagrams beneath the spectra in Figure 5, are based on results from homonuclear and heteronuclear correlation NMR experiments (^{11}B{^{19}F}−^{11}B{^{19}F}COSY,[42,43] ^{19}F{^{11}B}−^{19}F{^{11}B} COSY, ^{11}B{^{19}F}−^{19}F{^{11}B} 2D), and chemical shifts derived from DFT-GIAO calculations.

Because of the partially overlapping signals in the ^{11}B NMR spectrum of anions **3** and **4**, the information gained from ^{11}B{^{19}F}−^{11}B{^{19}F} COSY spectra is limited (Figure S3−S5 in the Supporting Information). However, the cross-peaks in the ^{11}B 2D NMR spectrum of **2** in Figure S3 (Supporting Information) allow the unequivocal assignment of the signals, in agreement with the order predicted by DFT-GIAO calculations (Table 3).

Although ^{19}F−^{19}F COSY experiments are routine experiments for the analysis of highly fluorinated compounds,[44] to our knowledge such studies have not been reported for fluorine-substituted boron compounds, so far. Unfortunately, for nearly all of the signals, cross-peaks are observed in the ^{19}F{^{11}B} 2D spectra of the three aminocarborate anions; hence, an additional support for the assignment of the ^{19}F NMR signals is not obtained. Probably, this finding is explained by large ^4J, and in addition, weaker ^3J and ^5J couplings between the ^{19}F nuclei, as generally found in fluorocarbon compounds, resulting in correlations between nearly all of the fluorine nuclei in the *closo*-carborate anions.[44] Further work on carborate anions with less fluorine atoms might help to better understand the ^{19}F−^{19}F couplings.

Heteronuclear correlation spectroscopy experiments of ^{1}H and ^{11}B are standard methods for the characterization of boranes and borates since the early 80s of the last century,[45,46] but analogous measurements involving the nuclei ^{11}B and ^{19}F do not seem to be reported in the literature.[44] The ^{11}B-{^{19}F}−^{19}F{^{11}B} 2D experiments finally enabled the assignments of all of the ^{11}B and ^{19}F signals in the spectra of **2**, **3**, and **4** (Figure 6).

The most-simple ^{11}B and ^{19}F NMR spectra are observed for **2**, each exhibiting three signals with an intensity distribution of 1:5:5 due to the C_{5v} local symmetry of the 12-vertex cluster in solution. Whereas the assignment of the signals with a relative intensity of one for the antipodal B−F unit is unambiguous from the 1D NMR experiments, the other assignments are based on the ^{11}B{^{19}F}−^{11}B{^{19}F} COSY and the ^{11}B{^{19}F}−^{19}F{^{11}B} 2D NMR measurements (Figure 6, and Figure S3 in the Supporting Information). The ^{11}B NMR chemical shift increases with increasing distance from the carbon atom in the cluster. According to experimental, as well as to theoretical data in the ^{19}F NMR spectrum, a

(42) Venable, T. L.; Hutton, W. C.; Grimes, R. N. *J. Am. Chem. Soc.* **1982**, *104*, 4716.
(43) Venable, T. L.; Hutton, W. C.; Grimes, R. N. *J. Am. Chem. Soc.* **1984**, *106*, 29.
(44) Battiste, J.; Newmark, R. A. *Prog. Nucl. Magn. Reson. Spectrosc.* **2006**, *48*, 1.
(45) Colquhoun, I. J.; McFarlane, W. *J. Chem. Soc., Dalton Trans.* **1981**, 2014.
(46) Finster, D. C.; Hutton, W. C.; Grimes, R. N. *J. Am. Chem. Soc.* **1980**, *102*, 400.

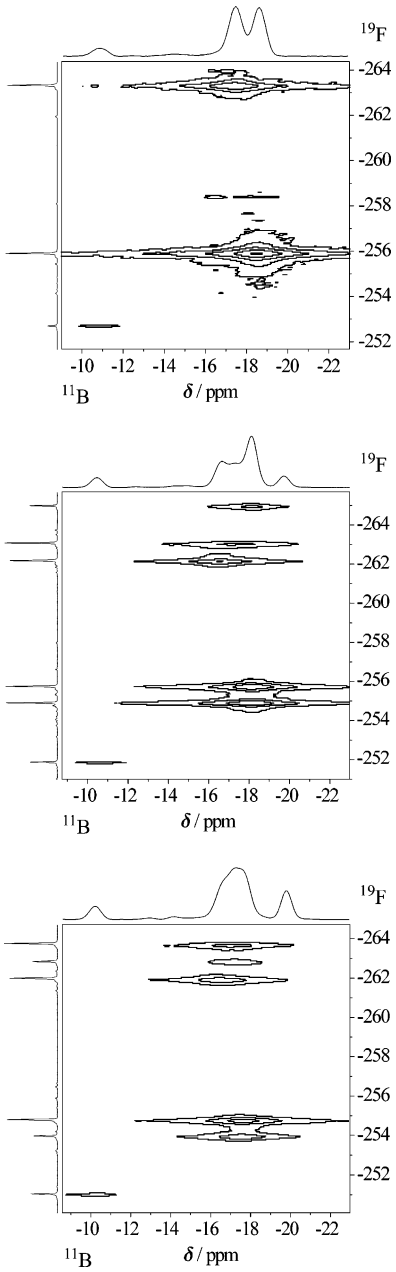

Figure 6. $^{11}B\{^{19}F\}-^{19}F\{^{11}B\}$ 2D NMR spectra of **2** (top), **3** (middle), and **4** (bottom).

different trend is observed: $\delta(^{19}F)$ increases in the order F7−F11 (upper belt) < F2−F6 (lower belt) < F12 (antipodal). Related trends in $\delta(^{11}B)$ and $\delta(^{19}F)$ are found for [1-H−$CB_{11}F_{11}]^-$ (Table 3). A similar tendency of the chemical shift of the boron nuclei in the nonfluorinated anion [1-H−$CB_{11}H_{11}]^-$ is also observed (Table 3).[16] For **1**, a different behavior for $\delta(^{11}B)$ was reported with the order B2−B6 > B7−B11 ≈ B12,[15] in good agreement to calculated chemical shifts B2−B6 > B12 > B7−B11. Interestingly, $\delta(^{11}B)$ of the iodinated anion [1-$H_2N-CB_{11}I_{11}]^-$ displays an intermediate behavior: B12: −11.8 ppm, B2−B11: −14.8 ppm.[11]

All six ^{19}F NMR signals of the side product [1-H_2N-6-H−$CB_{11}F_{10}]^-$ are experimentally observed, whereas some of the ^{11}B NMR signals are covered by signals of anion **2** (Table 3). Assignments are based on calculated ^{19}F and ^{11}B chemical shifts with the exception of $\delta(^{11}B)$ of the B−H unit. In this case, the assignment is unambiguous from a splitting of the signal into a doublet due to $^1J(^1H,^{11}B)$ coupling (153 Hz). The strong shift of $\delta(^{11}B)$ of the B−H group to a negative value (−36.0 ppm) in comparison to the signals of **1** is typical because $\delta(^{11}B)$ for BH groups decreases with increasing degree of fluorination in *closo*-carborate[4,32] and *closo*-borate anions.[47−49] Although further signals of low intensity (<2%) are found in the $^{19}F\{^{11}B\}$ NMR spectrum of **2**, an unambiguous assignment to the most-probable side products [1-H_2N-4,6-$H_2-CB_{11}F_9]^-$ and/or [1-H_2N-5,6-$H_2-CB_{11}F_9]^-$ was not achieved, so far.

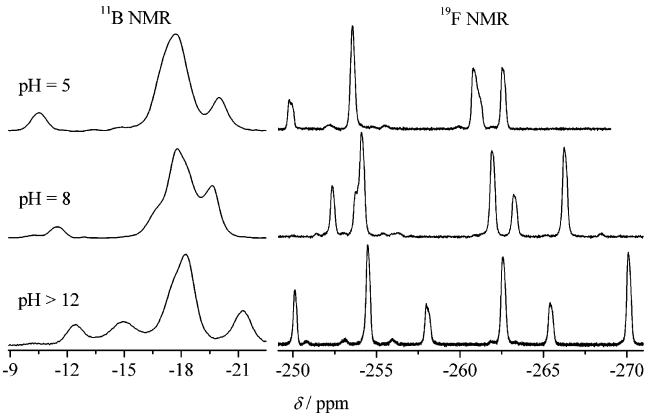

Figure 7. ^{11}B and ^{19}F NMR spectra of **4** in D_2O at different pH values.

The assignments of $\delta(^{11}B)$ and $\delta(^{19}F)$ of **3** and **4** as given in Table 3 and illustrated in Figure 5 are based on experimental, especially $^{11}B\{^{19}F\}-^{19}F\{^{11}B\}$ 2D data (Figure 6), supported by theoretical values. The order of the nuclei in the upper belt, lower belt, and the antipodal position, as found for the parent anion **2**, is retained, as shown in the stick diagrams below the spectra in Figure 5. The average ^{11}B and ^{19}F chemical shifts of the B−F units in these three different regions slightly increase with an increasing number of hydroxy groups. Cross signals were not observed in the $^{11}B\{^{19}F\}-^{19}F\{^{11}B\}$ 2D signals for the signals of the ^{11}B nuclei attached to the hydroxy groups in **3** and **4**. These boron nuclei have lower chemical shifts compared to the respective nuclei in the parent anion **2**.

In Figure 7, the ^{11}B and ^{19}F NMR spectra of dihydroxy-substituted anion **4** at different pH values (5, 8, and >12) are depicted. With increasing pH, all of the ^{19}F NMR signals are shifted to lower frequencies with the exception of the fluorine atom bonded to B5, which is located between both B−OH groups. Calculated ^{19}F chemical shifts for the [1-H_2N-4-O-6-HO−$CB_{11}F_9]^{2-}$ dianion are in good agreement with experimental values at pH > 12 (Figure S9 in the Supporting Information). Hence, in concentrated aqueous potassium hydroxide, **4** is probably deprotonated. As a result of broad signals in the ^{11}B NMR spectra (Figure 7), a detailed analysis of the pH dependency of $\delta(^{11}B)$ is not possible, but the

(47) Solntsev, K. A.; Mebel', A. M.; Votinova, N. A.; Kuznetsov, N. T.; Charkin, O. P. *Koord. Khim.* **1992**, *18*, 340.
(48) Solntsev, K. A.; Ivanov, S. V.; Sakharov, S. G.; Katser, S. B.; Chernyavskii, A. S.; Votinova, N. A.; Klyuchishche, E. A.; Kuznetsov, N. T. *Russ. J. Coord. Chem.* **1997**, *23*, 369.
(49) Ivanov, S. V.; Lupinetti, A. J.; Solntsev, K. A.; Strauss, S. H. *J. Fluorine Chem.* **1998**, *89*, 65.

spectra indicate a comparable trend to higher frequencies as found for $\delta(^{19}F)$. The ^{11}B and ^{19}F NMR spectra of the monohydroxy species **3** at pH > 12 (Figure S10 in the Supporting Information) differ from the spectra measured in CD_3CN under neutral conditions (Figure 5) in a manner similar to those of related **4**. Especially, the strong shift to a lower $\delta(^{11}B)$ for the boron nucleus in the antipodal position under strongly basic conditions, similar to **4** (Figure 7), is remarkable.

Experimental and calculated ^{13}C chemical shifts of the *closo*-carborate anions **2**, $[1\text{-H}-CB_{11}F_{11}]^-$, and their nonfluorinated analogues agree very well (Table 4). $\delta(^{13}C)$ is shifted to lower values for the fluorinated anions. The ^{13}C chemical shift of the carbon nucleus in $[1\text{-}H_2N\text{-}6\text{-H}-CB_{11}F_{10}]^-$ is larger compared to $[1\text{-}H_2N-CB_{11}F_{11}]^-$, indicating a steady decrease in $\delta(^{13}C)$ with an increasing number of fluorine atoms.

A definite assignment of the ^1H NMR signals of protons in the amino and hydroxy substituents was not possible.

The largest $^1J(^{11}B,^{19}F)$ coupling constants in all of the *closo*-carborate anions described in this publication are found for the antipodal B−F units with values of approximately 60 Hz. A detailed comparison of the coupling constants derived from ^{19}F NMR spectroscopy is arbitrary because these numbers are uncertain due to the interaction with the quadrupolar ^{11}B nucleus, as evident from partial distortion of the signals (Figure 5).[50−52]

Vibrational Spectroscopy. Three modes of the $C-NH_2$ fragment: $\nu_{as}(NH_2)$, $\nu_s(NH_2)$, and $\delta(NH_2)$ are assigned in the vibrational spectra of K^+**2** to bands at 3390, 3331, and 1614 cm^{-1}, respectively (Figure 8). These values are close to those derived from DFT calculations at the B3LYP/6-311++G(d,p) level of theory (3595, 3511, and 1652 cm^{-1}). All three bands are shifted to slightly higher values in comparison to the respective wavenumbers of the nonfluorinated species K^+**1**: 3371, 3309, and 1583 cm^{-1} (Calcd: 3582, 3504, and 1648 cm^{-1}).

In the IR spectrum of K^+**2**, the most-intense bands correspond to the C−F stretches in the region of 1170−1380 cm^{-1}, very similar to the IR spectrum of $Cs[1\text{-H}-CB_{11}F_{11}]$ (Figure 8). The Raman intensities of these vibrations are zero, whereas the B−H stretches in K^+**1** are active in the IR and Raman spectra, similar to the parent anion $[1\text{-H}-CB_{11}H_{11}]^-$ in its Cs^+ salt.[53] Bands of low intensity at approximately 2600 cm^{-1} in the Raman spectra of K^+**2** and $Cs[1\text{-H}-CB_{11}F_{11}]$ indicate the presence of small amounts of anions with residual hydrogen atoms, in agreement with results from NMR spectroscopy and MALDI mass spectrometry.

The CH stretch in the vibrational spectra of $Cs[1\text{-H}-CB_{11}F_{11}]$ is unambiguously assigned to the band at 3028 cm^{-1}. With the aid of calculated wavenumbers and a comparison to the spectra of K^+**2**, the band at 1017 cm^{-1} can be attributed to δ(CH).

The IR and Raman spectra of K^+**2** and $Cs[1\text{-H}-CB_{11}F_{11}]$ are very similar, apart from the modes of the $C-NH_2/C-H$ fragment, respectively (Figure 8), whereas a comparison to the spectra of K^+**1** and to the data reported for $Cs[1\text{-H}-CB_{11}H_{11}]$[53] exhibits considerable differences.

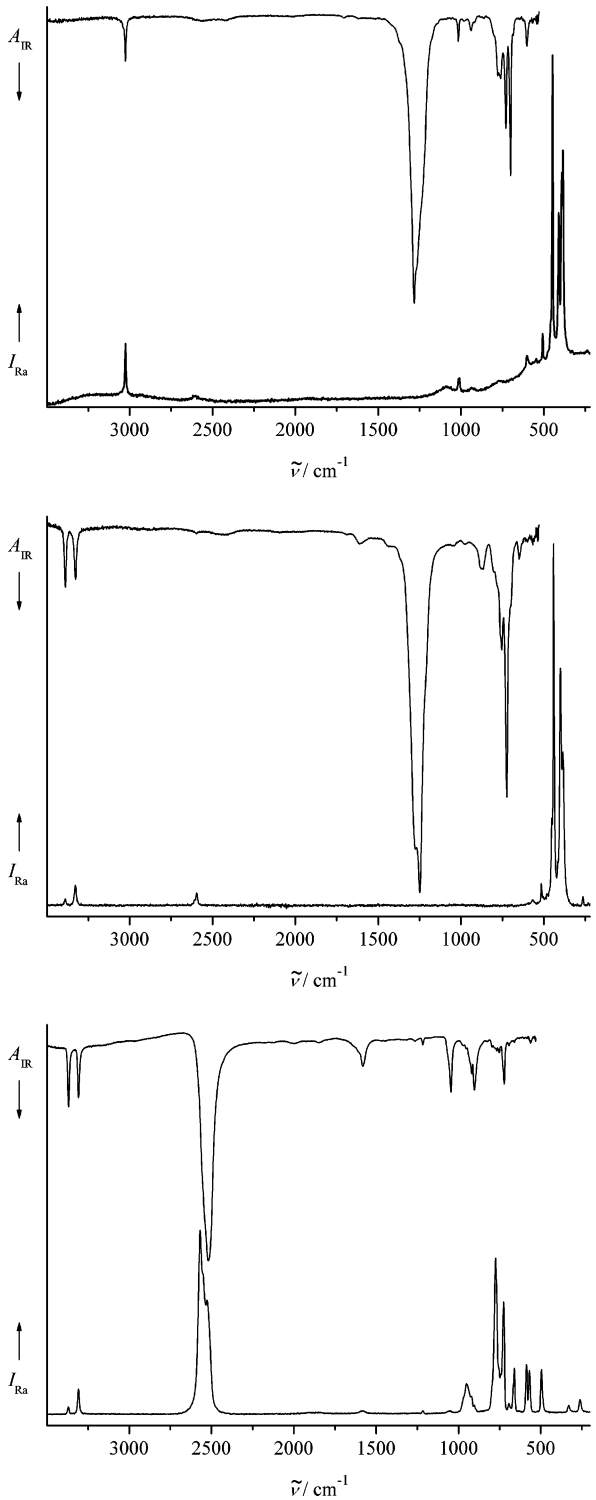

Figure 8. IR and Raman spectra of $Cs[1\text{-H}-CB_{11}F_{11}]$ (top), K^+**2** (middle), and K^+**1** (bottom).

(50) Halstead, T. K.; Osment, P. A.; Sanctuary, B. C.; Tangenfeldt, J.; Lowe, I. J. *J. Magn. Reson.* **1986**, *67*, 267.
(51) Wrackmeyer, B. In *Annu. Rep. NMR Spectrosc.*; Webb, G. A., Ed.; Academic Press Limited: London, U.K., 1988; Vol. 20, p 61.
(52) Abragam, A. *Principles of Nuclear Magnetism*; Clarendon Press: Oxford, U. K., 1986.
(53) Kononova, E. G.; Bukalov, S. S.; Leites, L. A.; Lyssenko, K. A.; Ol'shevskaya, V. A. *Russ. Chem. Bull., Int. Ed.* **2003**, *52*, 85.
(54) Patmore, N. J.; Hague, C.; Cotgreave, J. H.; Mahon, M. F.; G., F. C.; Weller, A. S. *Chem.—Eur. J.* **2002**, *8*, 2088.

The Raman and IR spectra of the $[Ph_4P]^+$ salts of hydroxy-substituted anions **3** and **4** are shown in Figures S11 and S12 in the Supporting Information. The IR spectra of both salts exhibit bands unambiguously assigned to ν(OH) 3490−3680 cm^{-1}, $\nu(NH_2)$ 3430−3310 cm^{-1}, and ν(CF) 1390−1160 cm^{-1} bands. A further interpretation is hampered because of cation bands.

Summary and Conclusions

The reaction of K[1-H_2N−$CB_{11}H_{11}$] (K^+**1**) with elemental fluorine in anhydrous HF to give K[1-H_2N−$CB_{11}F_{11}$] (K^+**2**) is the first example of a fluorination of a carba-*closo*-dodecaborate anion with a substituent other than hydrogen bonded to carbon. Contrary to the [1-H−$CB_{11}F_{11}$]$^-$ anion,[1] its amino congener **2** decomposes in aqueous acids. A similarity of both anions is the formation of a monohydroxy- and dihydroxy-substituted cluster: [1-R-$CB_{11}F_{10}$(OH)]$^-$ and [1-R-$CB_{11}F_9(OH)_2$]$^-$ (R = H, H_2N).[1]

Data from diffraction studies on single crystals of $[BzPh_3P]^+$**2** and $[Ph_4P]$[1-H_2N-4,6-$(HO)_2$−$CB_{11}F_9$] ($[Ph_4P]^+$**4**) together with bond parameters derived from DFT calculations give an insight into the bonding situation of the novel cluster anions. The most important result, an expansion of the cluster upon fluorination, is in agreement with previous experimental and theoretical studies on the parent system [1-H−$CB_{11}F_{11}$]$^-$. This behavior is reasoned by an elongation and hence weakening of the bonds between the carbon and boron atoms building the cluster framework.[10,31]

NMR spectroscopic characterization of the three *closo*-carborate anions is achieved by a combination of 1D and 2D ^{11}B and ^{19}F NMR spectroscopic measurements, which to our knowledge in this combination is unique for fluorinated carboranes and carborates. The assignment of the signals is further ensured by a comparison to calculated chemical shifts.

Acknowledgment. Financial support by the Fonds der Chemischen Industrie (FCI) is acknowledged. Furthermore, we are grateful to Merck KGaA, Darmstadt (Germany), for financial support and chemicals used in this work, to Solvay GmbH, Hannover (Germany), for a gift of elemental fluorine, and to BASF AG, Ludwigshafen (Germany) for a gift of BF_3·OEt_2. We are grateful to Professor W. Frank (Heinrich-Heine-Universität Düsseldorf) for generous support and thank Professor H. Willner (Bergische-Universität-Wuppertal) for allowing the use of equipment needed for handling of anhydrous HF and elemental fluorine. We thank Ms. E. Hammes, Mr. P. Roloff, and Dr. P. Tommes for technical support.

Supporting Information Available: MALDI mass spectra of [1-H_2N−$CB_{11}H_{11-n}F_n$]$^-$ (n = 3−11), **3**, and **4**, ^{11}B{^{19}F}−^{11}B{^{19}F} COSY and ^{19}F{^{11}B}−^{19}F{^{11}B} COSY NMR spectra of **2**, **3**, and **4**, ^{11}B and ^{19}F NMR spectra anion **3** in D_2O at pH > 12, a stick diagram displaying the calculated NMR chemical shifts of **4**, and IR and Raman spectra of $[Ph_4P]^+$**3** and $[Ph_4P]^+$**4**. X-ray crystallographic files in CIF format for K^+**2**, $[BzPh_3P]^+$**2**, $[Ph_4P]^+$**3**, $[Ph_4P]^+$**4**, and $[BzPh_3P]^+$**1**. This material is available free of charge via the Internet at http://pubs.acs.org.

IC701398U